Available online at www.sciencedirect.com
ScienceDirect
Ceramics International 35 (2009) 3027–3036
CERAMICS INTERNATIONAL
www.elsevier.com/locate/ceramint

The effect of nano-sized BNBT on microstructure and dielectric/piezoelectric properties

Man-Soon Yoon [a,*], Neamul Hayet Khansur [a], Byung-Ki Choi [b], Young-Geun Lee [a], Soon-Chul Ur [a]

[a] Dept. of Materials Sci. and Eng., Research Center for Sustainable Eco-Devices and Materials (ReSEM), Chungju National University, Chungbuk, 380-702, Republic of Korea
[b] Dept. of Research Center, CQV Co., Ltd., 27-5, Republic of Korea

Received 9 February 2009; received in revised form 20 March 2009; accepted 10 April 2009
Available online 21 May 2009

Abstract

$(Bi_{0.5}Na_{0.5})_{0.94}Ba_{0.06}TiO_3$ (abbreviated as BNBT6) ceramic of near MPB composition was synthesized by two different processes. The first one is the addition of pre-synthesized $BaTiO_3$ and pre-milled Bi_2O_3, Na_2CO_3, $BaCO_3$ powders and calcination powder milled with a high energy milling machine in order to obtain a nano-particle size. The second one is a conventional one to compare with the former process. The pre-milling and the pre-synthesis process of raw materials lowered the calcination temperature to the extent of 59 °C as compared with conventionally fabricated BNBT6. The particle size of the powder exposed to heavy high energy milling reduced to 50–70 nm, whereas that of the conventionally ball-milled powder without the pre-milling and the pre-synthesis process had a larger size of ~280 nm. To investigate the effects of the modified process on the characteristic of BNBT6 ceramics, the dielectric and the piezoelectric properties of sintered specimens fabricated by the two different processes were evaluated. It was found that the properties of the nano-sized BNBT6 ceramic near the MPB composition were increased by the modified mixing and milling method, showing superior characteristics in terms of the piezoelectric/dielectric constant and sintering density compared with those of the conventional process. The modified mixing and milling method was considered to be a new and promising process for lead-free piezoelectric ceramics owing to their excellent piezoelectric/dielectric properties.

Keywords: C. Piezoelectric properties; C. Dielectric properties; Pre-milling; Nano-sized BNBT

1. Introduction

Perovskite piezoelectric ceramics containing lead oxide such as Pb(Ti, Zr)O_3 (PZT), are now widely used in piezoelectric devices because of their excellent piezoelectric properties [1]. However, recently emerged environmental issues, such as the restriction of WEEE (Waste Electrical and Electronic Equipment) and RoHS (Restriction of Hazardous Substances), will prohibit us from using lead oxide in the near future due to their toxicity. In an approach to acclimate ourselves to recent ecological consciousness trends [2,3], a lead-free piezoelectric material, bismuth sodium barium titanate, was considered as an environment-friendly alternative for a PZT system.

Since bismuth sodium titanate, $Bi_{0.5}Na_{0.5}TiO_3$ (abbreviated as BNT), was discovered by Smolenskii and Agranovskaya in 1960 [4], BNT is considered to be an excellent candidate as a key material of lead-free piezoelectric ceramics because BNT is strongly ferroelectric. Besides, pure BNT shows a characteristic of diffuse phase transition (DPT). The BNT exhibits a large remnant polarization, P_r = 38 μC/cm^2, a high Curie temperature (T_c = 320 °C). The dielectric properties display also an interesting anomaly wherein a low temperature phase transition at 200 °C marks the transition from ferroelectric to antiferroelectric [5]. However, because of its high coercive field, E_c = 73 kV/cm, and relatively large conductivity, the pure BNT is difficult to be poled and cannot be a good piezoelectric material. These problems were then improved by forming solid solutions with $BaTiO_3$(BT), $Bi_{0.5}K_{0.5}TiO_3$, $KNbO_3$, $NaNbO_3$, $(Sr_aPb_bCa_c)$-TiO_3, $BiFeO_3$, $BiScO_3$, etc. [6–13]. Among these systems, bismuth sodium barium titanate $(Bi_{0.5}Na_{0.5})_{1-x}Ba_xTiO_3$ (BNBT)

* Corresponding author.
E-mail addresses: msyoon@cjnu.ac.kr (M.-S. Yoon), scur@cjnu.ac.kr (S.-C. Ur).

0272-8842/$36.00.
doi:10.1016/j.ceramint.2009.04.016

has been widely investigated by many researchers [7,14,15]. Morphotropic phase boundary (MPB) of this solid solution system is near $x = 0.06$, where the materials show enhanced piezoelectric and dielectric performances. Takenaka et al. [7] have reported that the composition of $(Bi_{0.5}Na_{0.5})_{0.94}Ba_{0.06}TiO_3$, which is near the MPB, has relatively good piezoelectric properties of $k_p = 0.25$, $k_{31} = 0.19$, $d_{33} = 125$ pC/N. However, this composition has a higher coercive electric field and medium piezoelectric constant. These properties were afterward promoted by a few research groups [16–18]. It was believed that substitution at A site or B site may induce soft or hard properties in a piezoelectric material by forming cation or oxygen vacancies, respectively. Several kinds of cations such as La^{3+}, Nb^{5+}, Co^{3+}, Mn^{2+}, etc. were tested to further modify BNT-based piezoelectric ceramics [19–22]. Many researchers have investigated to improve the properties of BNBT ceramics either by modifying fabrication technique or by dopants.

The purpose of this present study is to control the size and morphology of starting powder and to pre-synthesize $BaTiO_3$ in order to increase the reaction activity. Another objective is to demonstrate the effect of nano-sized BNBT particles on the microstructure and the piezoelectric/dielectric properties.

2. Experimental procedure

Perovskite $(Bi_{0.5}Na_{0.5})_{0.94}Ba_{0.06}TiO_3$ (abbreviated as BNBT6) ceramics were fabricated by the two different processes. One is the process I, which contains the pre-milling process and the pre-synthesizing process of the starting powder and the high energy milling process of calcined powder [sometimes abbreviated as nano-sized BNBT6] and the other is the process II, which contains the conventional mixing and milling process [sometimes abbreviated as conventional BNBT6]. The detailed fabrication process was shown in Fig. 1. According to the process I, to effectively eliminate the problems associated with a size and morphology differences of raw materials, Bi_2O_3 (High purity chem. Co.), Na_2CO_3 (Cerac Co.) and $BaCO_3$ (Sakai chem. Co.) among the starting materials were the first pre-milled in ethanol using a ball-mill with 3 mm ZrO_2 balls for 72 h. The second stage of the fabrication was synthesis of $BaTiO_3$. Stoichiometric amount of the pre-milled $BaCO_3$ and as-received anatase phase TiO_2 with 100 nm size were mixed in ethanol using a ZrO_2 media. The dried powder was then calcined at 950 °C for 2 h in an alumina crucible. X-ray analysis was performed at this stage. The pre-milled Bi_2O_3, Na_2CO_3, the pre-synthesized $BaTiO_3$ powders and as-received TiO_2 (Tronox: anatase) were then ball-milled in ethanol using a ZrO_2 media for 24 h. Mixed powder was calcined at 720 °C for 4 h. X-ray analysis was also performed at this stage and the calcination temperature was selected by means of TG/DTA analysis. After calcining, an additional milling step with nano-mill (MINICER/MINIPUR-NETZSCH) was added to obtain a nano-particle size. Milling was conducted in ethanol with zirconium balls of 0.2 mm diameter for 1 h with rotor speed of 3500 rpm.

To compare the properties of nano-milled BNBT6 powder with those of conventionally prepared BNBT6 powder, BNBT6

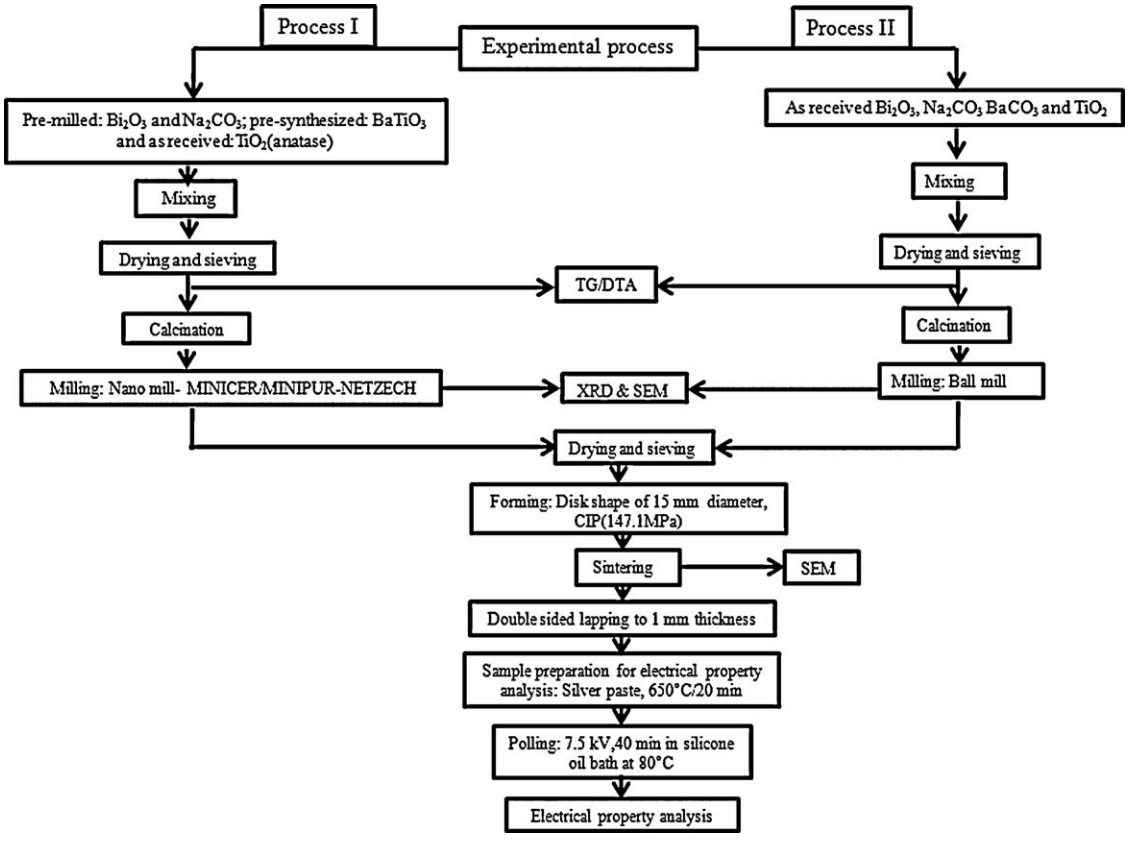

Fig. 1. Processing block diagram for BNBT preparation (process I: nano-sized BNBT6 and process II: conventional BNBT6).

powder having the same composition with process I was fabricated by using a conventional ball-mill process. Raw materials of analytical-reagent (AR) grade Bi_2O_3, Na_2CO_3, $BaCO_3$, rutile phase TiO_2 were weighed and ball-milled with a ZrO_2 media in ethanol for 24 h. The dried powder was then calcined at 850 °C for 4 h. An additional ball-milling step of the calcined powder was added to ensure a fine particle size. The dried powders, which are prepared by using the two different processes, were then pressed as a disk of 15 mm diameter and then cold-isostatically pressed under 147.1 MPa. The pressed samples were sintered at various temperatures for 2 h. The sintered samples were then polished to obtain parallel surface up to 1 mm of thickness. Powder morphologies and microstructures of the all samples were investigated using a scanning electron microscope (SEM; FEI Company Quanta400). In order to measure the electrical properties, silver paste was coated to form electrodes on both sides of the sample, and then subsequently fired at 650 °C for 20 min. The dielectric and

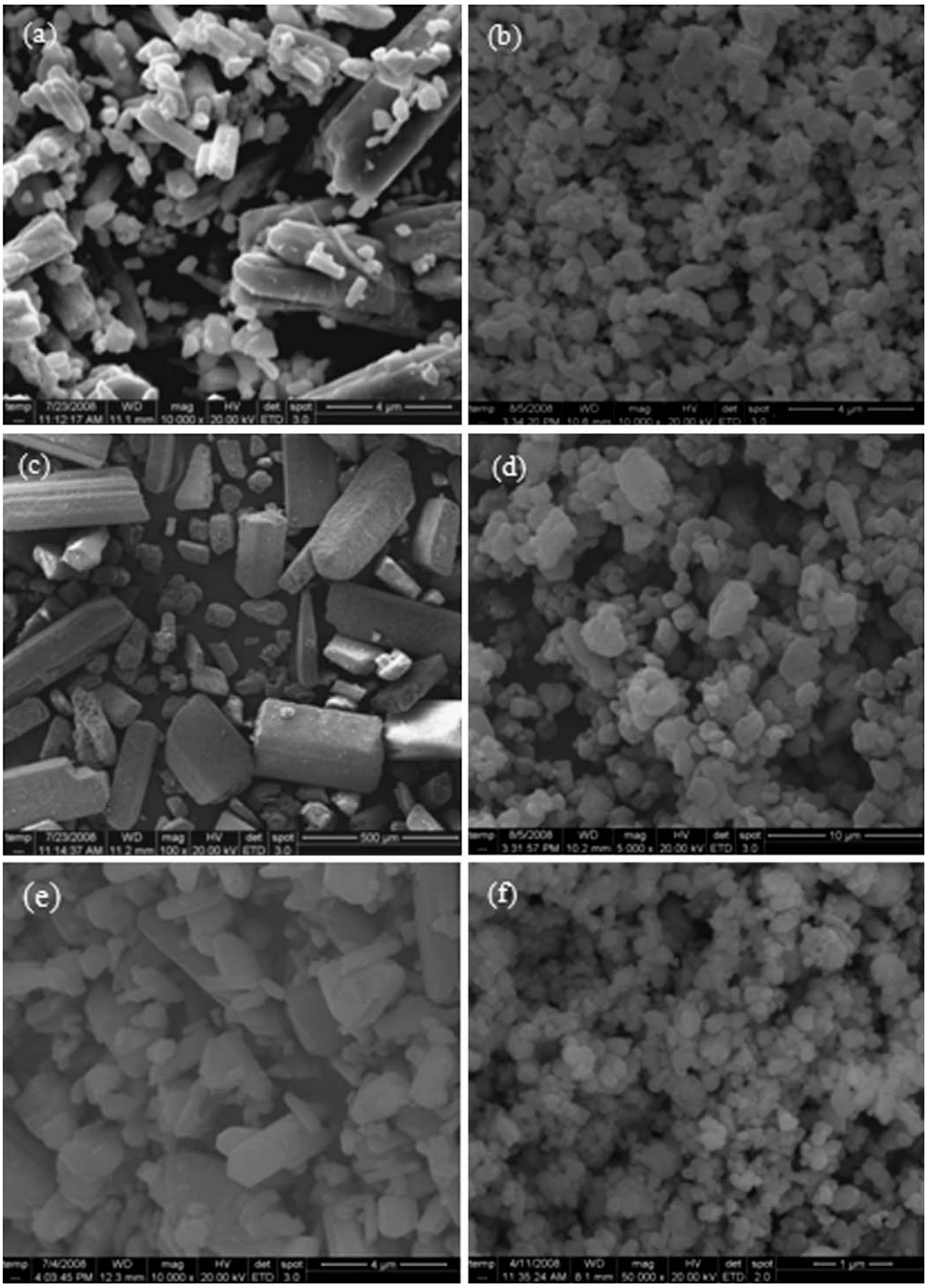

Fig. 2. SEM micrographs of the starting materials used in the synthesis of BNBT: (a) as-received Bi_2O_3, (b) 72 h ball-milled Bi_2O_3, (c) as-received Na_2CO_3, (d) 72 h ball-milled Na_2CO_3, (e) as-received $BaCO_3$, and (f) 72 h ball-milled $BaCO_3$.

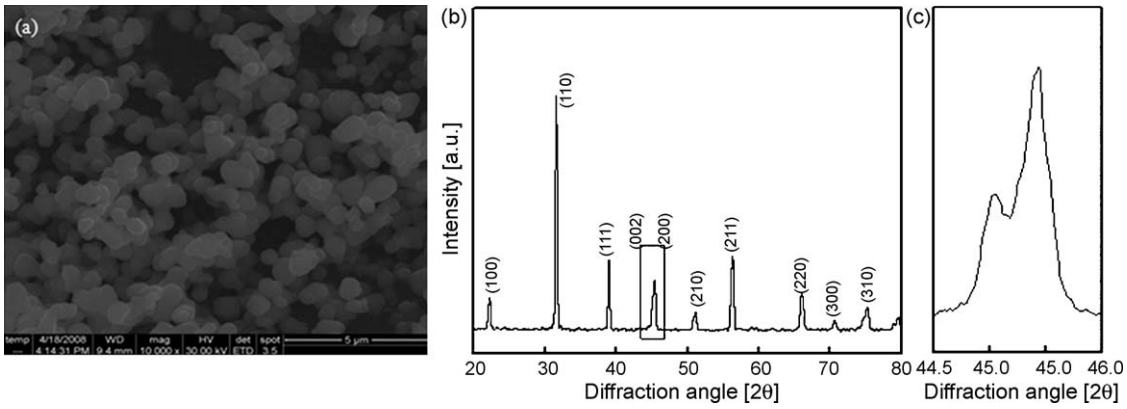

Fig. 3. The powder morphology and X-ray diffraction patterns of pre-synthesized $BaTiO_3$: (a) SEM micrograph (b) X-ray diffraction patterns, and (c) {2 0 0} reflection.

the piezoelectric properties were measured using an impedance/gain phase analyzer (HP-4194A) after poling under 7.5 kV/mm at 80 °C in a silicone oil bath for 40 min. Piezoelectric properties were calculated to use a resonance/anti-resonance measurement method [23]. To obtain *P–E* hysteresis curve, the induced electric polarization at room temperature was measured using a Precision LC system (Radiant Technology Model: 610E).

The phase-formation characteristics and tetragonality of *c/a* were determined using X-ray diffraction (XRD) patterns and the multi-peak separation method (Jandal Scientific PEAKFIT, version 3.18).

3. Results and discussion

3.1. Effects of pre-milled starting powders and pre-synthesized $BaTiO_3$ on the reaction temperature and the crystal structure

Fig. 2 shows the SEM micrograph of as-received and pre-milled Bi_2O_3, Na_2CO_3, and $BaCO_3$, exclusive of the TiO_2 powder having fine and sphere type particle morphology (average particle size: 100 nm). It has been reported that fine particles of TiO_2 act as a catalyst for the decomposition of carbonate [24], and the anatase-phased TiO_2 has a higher activity and is more efficient in lowering reaction temperature than the rutile one due to its low density (density of anatase phase $TiO_2 = 3.90\ g/cm^3$, while that of the rutile phase = 4.23 g/cm^3) [25]. The purpose of the pre-milling stage by ball-milling is to increase contact points and activity of starting materials. From the micrograph results of the pre-milled powders, it is evident that the process causes a significant change in particle morphology, accompanying the powder shape change from a square pillar shape to a regular sphere shape. On the other hand, since a solid-state reaction method is the most traditional one for preparing $BaTiO_3$ powders by mixing the starting materials, usually titanium oxide and barium carbonate, and calcining them at an elevated temperature around 1100–1400 °C [26,27], the high reaction temperature of $BaTiO_3$ will be expected to severely inhibit the calcination reaction of BNBT6. Moreover, as the powder from this traditional method had been known to result in a significant amount of agglomeration and poor chemical homogeneity along with a coarse particle size due to the treatment at high temperature, the additional pre-process adopting the pre-milling of $BaCO_3$ was performed to ensure the fine particle size and decrease the reaction temperature. Therefore, the mixture of $BaTiO_3$ was prepared with the pre-milled $BaCO_3$ and as-received anatase phase TiO_2 of 100 nm size and then calcined at 950 °C. The calcined $BaTiO_3$ was then added to the mixing process of BNBT6 [as described in process I] in order to decrease the calcination temperature. The powder morphology and X-ray diffraction patterns of pre-synthesized $BaTiO_3$ were observed as shown in Fig. 3. The average particle size was 350 nm, showing the sphere and regular shape. Despite the lower reaction temperature of 950 °C, it is fully stabilized to perovskite structure without second and/or pyrochlore phases. In addition to this, (2 0 0) and (0 0 2) peaks were widely separated. The multi-peak separation method was used to estimate the tetragonality of the sample. For this purpose, the peak at $2\theta \sim 45^\circ$ was separated into two tetragonal peaks

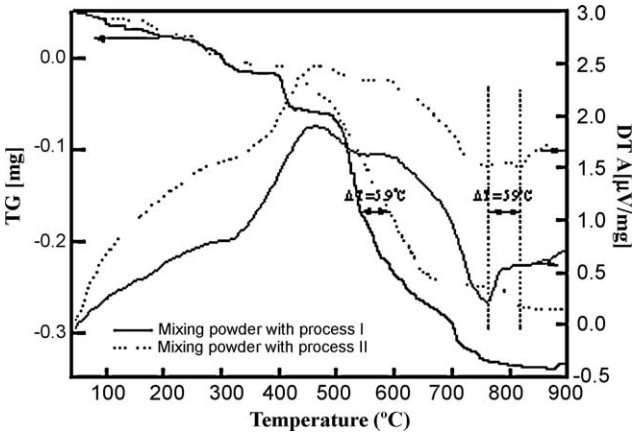

Fig. 4. Comparison of the solid-state reaction temperature using TG/DTA results among different processing in air with 3 °C/min of heating rate. The results of pre-milling and pre-synthesis process are marked as a solid line, and those of conventional process are marked as dash line.

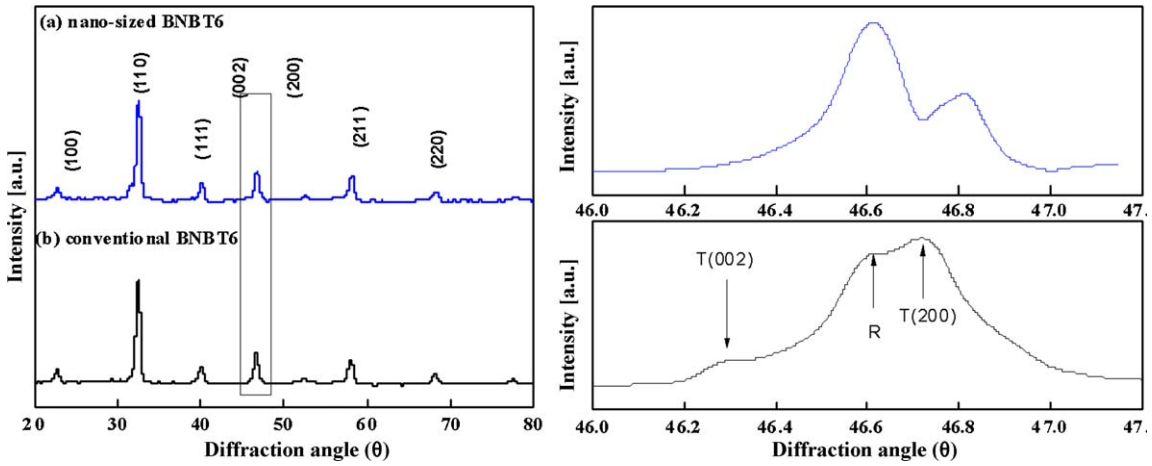

Fig. 5. X-ray diffraction patterns of nano-sized BNBT6: (a) conventional BNBT6 and (b) the X-ray diffraction patterns of {2 0 0} reflection.

[(2 0 0) and (0 0 2) planes] using Gauss–Cauchy function. The tetragonality is measured from lattice parameters of *c*- and *a*-axes which can be calculated by the following equation:

$$\frac{1}{d^2} = \frac{h^2 + k^2}{a^2} + \frac{l^2}{c^2} \quad (1)$$

From the results, a full stabilization of perovskite phase was achieved for pre-synthesized $BaTiO_3$ and the tetragonality was 1.007.

To observe the effect of the pre-milling and the pre-synthesis on the calcination temperature, the thermo-gravimetric/differential thermal analysis (TG/DTA analysis) is performed

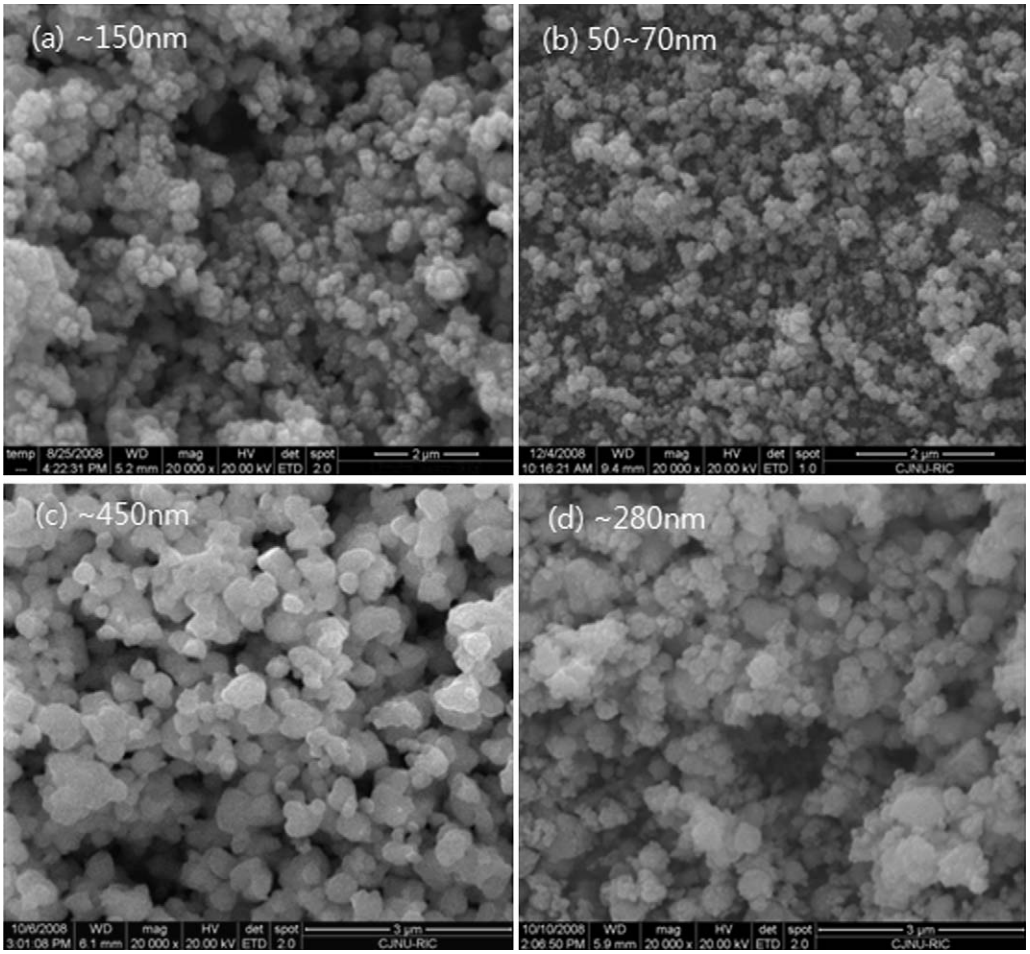

Fig. 6. The SEM morphology of calcined and milled powders: (a) and (b) calcined and nano-milled BNBT6 powder morphologies with pre-milling and pre-synthesis process (c) and (d) calcined and nano-milled BNBT6 powder morphologies without pre-milling and pre-synthesis process.

and the results are shown in Fig. 4. According to the (TG/DTA) results, the pre-milling process of the starting materials and the use of anatase phase TiO_2, pre-synthesis $BaTiO_3$ are effective in decreasing the reaction temperature by almost 59 °C compared to the powder without the pre-milling and the pre-synthesis processes as shown in Fig. 4.

Fig. 5 shows the X-ray diffraction patterns for the calcined BNBT6 samples, fabricated by the processes I and II, in the 2θ range of 20–80° and 46–47.2°. All of them are fully stabilized to perovskite structure without second and/or pyrochlore phases. All samples of BNBT6 show coexistence of tetragonal and rhombohedral symmetry. To observe the effect of the pre-milling and the pre-synthesis on the tetragonality, the multiple peak separation method was again used for the estimate of *c*/*a*. From the data of (0 0 2) peak, *c*/*a* for BNBT6 fabricated by the process II has a higher value of 1.0045 compared with 1.0039 of BNBT6 fabricated by the process I. The result of Fig. 5(b) indicates that the (0 0 2), (2 0 0) peaks of BNBT6 fabricated by the process I are suppressed and the rhombohedral phase increases. This result can be interpreted as the size effect.

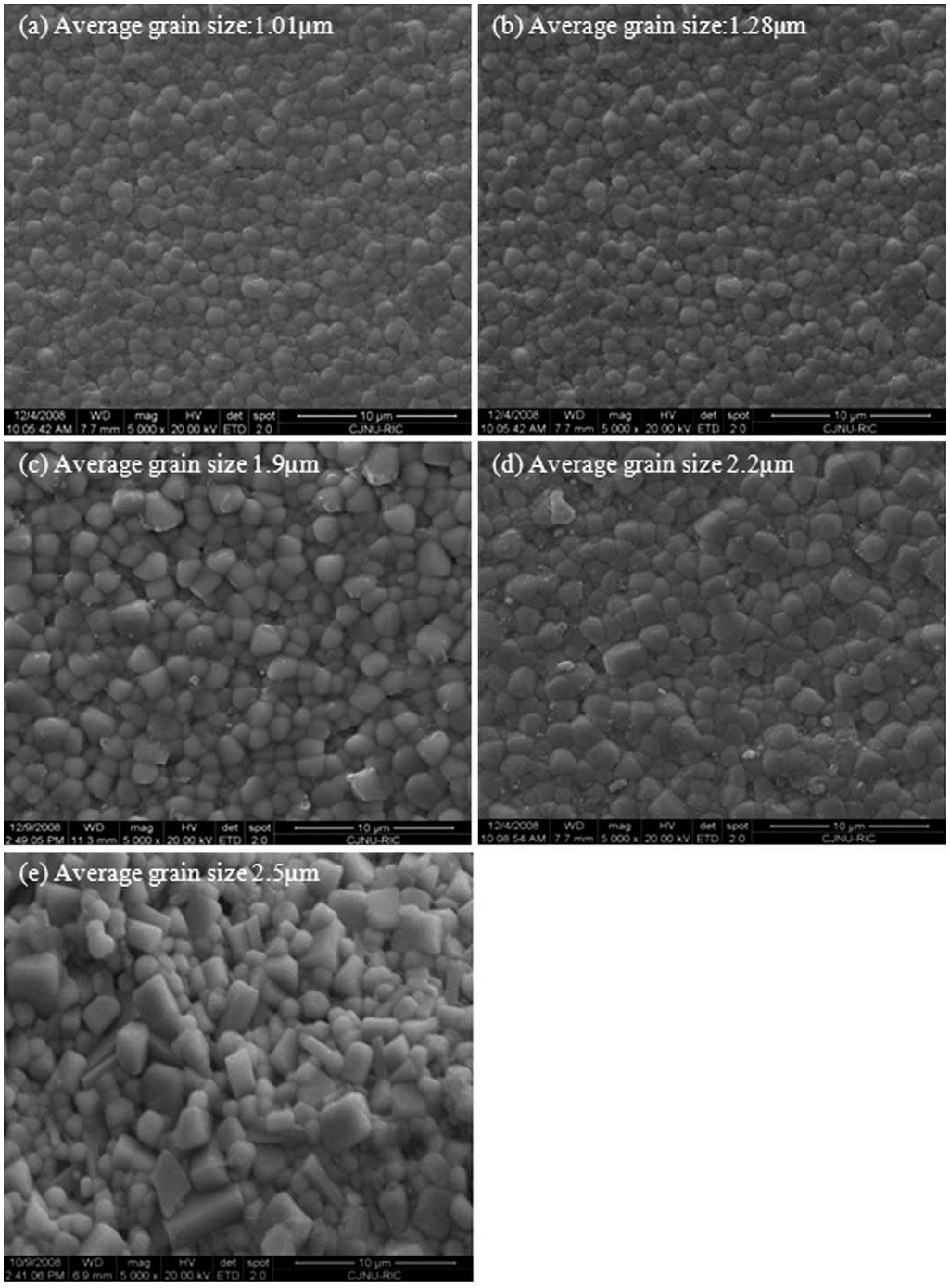

Fig. 7. SEM micrograph of nano-sized BNBT6 sintered at (a) 1100 °C, (b) 1130 °C, (c) 1170 °C, (d) 1190 °C for 2 h and (e) conventional BNBT6 sintered at 1170 °C for 2 h.

Similarly, Uchino et al. [28] interpreted the decrease of tetragonal phase in fine-grained $BaTiO_3$ as surface tension. According to them, this surface tension is sufficiently high to decrease the tetragonality in the fine particle sized $BaTiO_3$. More detailed report on the size effect was proposed by Begg et al. [29]. They reported that hydrothermal $BaTiO_3$ powder with a particle size larger than 270 nm was completely tetragonal and with a particle size less than 190 nm was a fully cubic phase. Since the pre-milling and the pre-synthesis lower the reaction temperature and then reduce the particle size to 160 nm as shown in the following subsection, it is highly probable that conventional BNBT6 powder fabricated by mixing the raw materials without any pre-processes (i.e. without adding the pre-milling and pre-synthesis process) has a higher tatragonality than that of the nano-sized BNBT6.

3.2. Effects of the nano-sized BNBT powder on the microstructure and the piezoelectric/dielectric properties

According to the previous results, the pre-milling and pre-synthesis processes lowered the calcination temperature of BNBT6, suggesting a decreased particle size of calcined powder and a change of the piezoelectric and dielectric properties. Fig. 6 shows the SEM morphology of the nano-milled and conventional ball-milled BNBT6 powders calcined at 720 °C and 850 °C, respectively. The sample calcined at 720 °C has a smaller average particle size of 150 nm compared with that of ~450 nm in the sample calcined at 850 °C. Furthermore, since the pre-milling and pre-synthesis processes induced a fine particle size and weakened neck growth, the particle size of the powder exposed to heavy high energy milling reduced to 50–70 nm, whereas that of conventionally ball-milled powder without the pre-milling and pre-synthesis process had a larger size of ~280 nm. It is evident that BNBT6 fabricated by the process I can reduce the particle size up to nano-scale. Therefore, it is expected that the fine starting material and the pre-synthesizing process of $BaTiO_3$ enhance the solid–solid reaction due to their high activity, and decrease the reaction temperature and the final particle size.

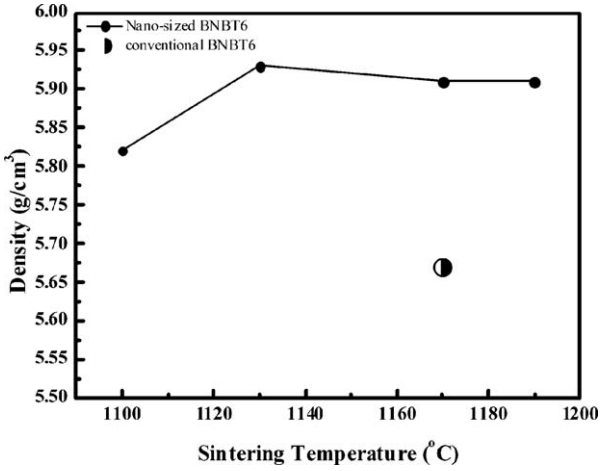

Fig. 8. The variations of density as a function of sintering temperature. The marked ◑ designates the density of conventional BNBT6 sample.

The microstructures of the sintered BNBT6 samples are observed by SEM. The micrographs of the nano-sized BNBT6 samples for various sintering temperatures are shown in Fig. 7(a)–(d), compared with conventional BNBT6 of Fig. 7(e). As shown in Fig. 7, grain shapes of the nano-sized BNBT6 are of polyhedral shape, while that of conventional BNBT6 is a square pillar shape. Furthermore, since the microstructure is directly associated with the sintering density, the variation densities of all samples are plotted in Fig. 8. As the results, the nano-sized specimen sintered at 1130 °C shows maximum values of the sintering density of 5.94 g/cm^3 compared to the nano-sized BNBT6 sample sintered at 1100 °C with 5.8 g/cm^3 and which then slightly decrease to 5.91 as increasing sintering temperature. On the other hand, conventional BNBT6 has a lower sintered density of 5.67 g/cm^3 than those of the nano-sized specimens. Therefore, the observed equilibrium shape change seems to be closely related with the increase of the sintering density.

To observe the effects of grain size on the piezoelectric and dielectric properties, the variation of these properties at the various sintering temperatures are plotted in Fig. 9(a) and (b). As shown in Fig. 9, the planar electromechanical coupling

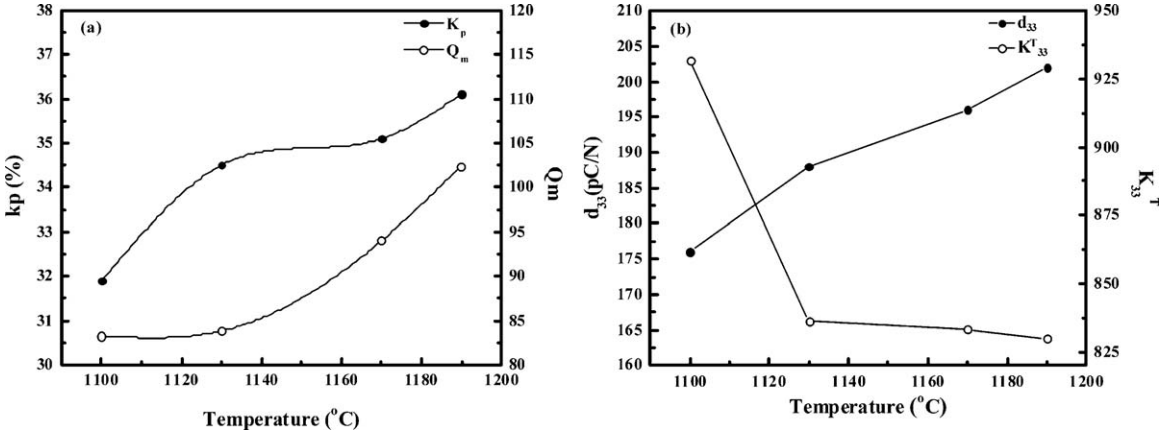

Fig. 9. Variation of piezoelectric and dielectric properties as a function of sintering temperature in nano-sized BNBT6: (a) planar electromechanical coupling factor (k_p) and mechanical quality factor (Q_m), (b) piezoelectric constant (d_{33}) and relative dielectric permittivity (K_T^{33}).

factor (k_p), the mechanical quality factor (Q_m) and the piezoelectric constant (d_{33}) of the nano-sized BNBT6 increase with increasing sintering temperature. However, the dielectric permittivity (K_T^{33}) sharply decreases just below 1130 °C, while it weakly depends on the sintering temperature above 1130 °C. The increase of Q_m, k_p and d_{33} can be interpreted as the effect of a grain size. Kang et al. [30] reported in $Pb_{0.9}La_{0.1}TiO_3$ system that poling efficiency increases with increasing the grain size, enhancing the facility of 90° domain switching. According to their result, since the increase of the grain size would be expected to enhance the domain switching at the same poling condition, the increases of k_p and d_{33} can be explained by the increased domain mobility. In addition to this, the increase of the grain size decreases the grain boundary, resulting in the decrease of grain boundary loss and this in turn increases Q_m with increasing the sintering temperature (Q_m is inversely proportional to loss tangent). On the other hand, the variation of the dielectric permittivity (K_T^{33}) is different from those of piezoelectric properties as shown in Fig. 9(b). Similarly, Arlt [31] reported that there was a transition region of the domain structure as a function of the grain size in the polycrystalline $BaTiO_3$. According to his paper, the domain remains a simple lamellar structure when the grain is small. As the grain size increases over some critical values, the structure is changed to a complex banded domain structure, accompanying the relaxation of the internal stress caused by tetragonal phase. Furthermore, Uchino [32] reported that PLZT showed the minimum value of K_T^{33} near the region where the domain structure was changed. It means that 90° twin caused by tetragonal phase cannot exist below the critical grain size, suggesting an increase of internal stress and which then anomalously increases K_T^{33} according to the model proposed by Bussem et al. [33,34]. As the sintering temperature increases above 1130 °C, the dielectric permittivity has almost same value. Similarly, Kang et al. [30] interpreted the phenomenon as transition region of the domain structure. They proposed that there were a microstructure transition region between the simple lamellar and the complex banded domain structure between 1.3 μm and 2.7 μm, therefore, K_T^{33} did not undergo sharp change.

Table 1
The comparison characteristics of the BNBT6 samples fabricated by two different processes.

Specimen	Density (g/cm^3)	d_{33} (pC/N)	K_T^{33}	k_p (%)	Q_m
Process I BNBT6	5.90	196.00	833.210	34.8	102
Process II BNBT6	5.67	152.02	671.526	31.3	73

Further evidence for the grain size effect was obtained by examining temperature dependence of *P–E* hysteresis curve at room temperature as shown in Fig. 10. The values of remnant polarization (P_r) and coercive field (E_c) were determined from the measured loops. From the data of hysteresis loops measured at room temperature, the remnant polarization P_r for BNBT6 sintered at 1100 °C specimen has a minimum value of 15.7 μC/cm^2, resulting in a lower value compared with the P_r of BNBT6 sintered at higher temperature [P_r = 37 μC/cm^2 for BNBT6 sintered at 1130 °C, P_r = 37.8 μC/cm^2 sintered at 1170 °C and 38.4 μC/cm^2 for BNBT6 sintered at 1190 °C] and the shape of loops corresponds to a typical polarization curve for a normal ferroelectric below the Curie temperature. In addition to this, the coercive field E_c for BNBT6 sintered at 1100 °C specimen has a maximum value of 36 kV/cm. Therefore, these results were in agreement with a previous analysis of the piezoelectric/dielectric properties as a clamping effect caused by internal stress below critical grain size.

To investigate the effects of manufacturing process on the piezoelectric and dielectric properties, the piezoelectric and dielectric properties of BNBT6 samples sintered at the same temperature, have been listed in Table 1. As the results, the piezoelectric and dielectric properties of nano-sized BNBT6 show the higher values compared with those of the conventional BNBT6. The observed increase of the piezoelectric and dielectric properties can be interpreted as the effects of the higher density and the coherency of grain boundary caused by an equilibrium shape.

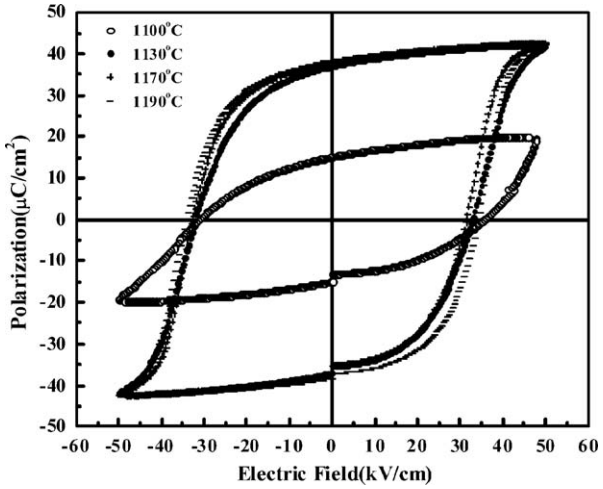

Fig. 10. Electric field-induced *P–E* hysteresis loops in nano-sized BNBT6 as a function of sintering temperature.

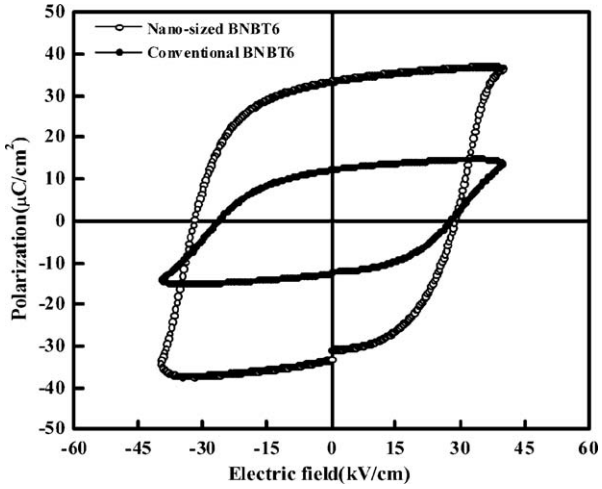

Fig. 11. The *P–E* curves for nano-sized BNBT6 and conventional BNBT6 at 25 °C.

Similarly, Haertling and Zimmer [35] reported that the dielectric constant and the piezoelectric properties increased with decreasing porosity of PZT ceramics. Therefore, it can be concluded that the process I increases the sintering density and decreases the porosity and this in turn accompanies the increase of the piezoelectric and dielectric properties.

Since the piezoelectric/dielectric properties are directly associated with a behavior of polarization–electric field (P–E) curve, the P–E curves for the nano-sized BNBT6 and conventional BNBT6 sintered at the same temperature are plotted in Fig. 11. The values of remnant polarization (P_r) and coercive field (E_c) were determined from the measured loops. From the data of hysteresis loops measured at 25 °C, the remnant polarization P_r for the nano-sized BNBT6 specimen has a higher value of 37.8 μC/cm^2 compared with that of 12 μC/cm^2 for conventional BNBT6; whereas the coercive field (E_c) has a similar value. These results were in agreement with the previous analysis of the piezoelectric/dielectric properties as a higher density caused by the equilibrium shape.

4. Conclusions

The effects of manufacturing process on the dielectric/piezoelectric properties and the microstructure in the BNBT6 ceramic were systematically investigated. The effects of the pre-milled starting powders and pre-synthesized $BaTiO_3$ on the reaction temperature and the crystal structure were examined by using BNBT6 in the MPB region. The results of thermo-gravimetric/differential thermal analysis (TG/DTA) revealed that the pre-milling process of starting materials and the use of anatase phase TiO_2 and pre-synthesis $BaTiO_3$ are effective in decreasing the reaction temperature by almost 59 °C compared to the powder without the pre-milling and pre-synthesis processes. From the X-ray analysis, all of the samples were fully stabilized to perovskite structure without second and/or pyrochlore phases. All samples of BNBT6 showed the coexistence of tetragonal and rhombohedral symmetry. From the data of (0 0 2) peaks, c/a for BNBT6 fabricated by the process II had a higher value of 1.0045 compared with 1.0039 of BNBT6 fabricated by the process I. This result could be interpreted as the size effect. The average particle sizes of the samples calcined at two different temperatures was 140–160 nm and ∼450 nm, respectively. Furthermore, since the pre-milling and pre-synthesis processes induced a fine particle size and weakened neck growth, the particle size of the powder exposed to the heavy high energy milling reduced to 50–70 nm, whereas that of conventionally ball-milled powder without the pre-milling and pre-synthesis process had a larger size of ∼280 nm. It was evident that BNBT6 fabricated by the process I can reduce the particle size up to nano-scale. From the microstructures analysis, applying the process I led grain shape to change from a square pillar shape to a polyhedral shape, accompanying the increase of sintered density. The piezoelectric and dielectric properties of the nano-sized BNBT6 could be interpreted as the grain size effect. Furthermore, the piezoelectric and dielectric properties of the nano-sized BNBT6 had higher values as compared with conventional BNBT. Further examination of the remnant polarization P_r for the nano-sized BNBT6 specimen showed a higher value of 37.8 μC/cm^2 compared with that of 12 μC/cm^2 for conventional BNBT; whereas the coercive field (E_c) has a similar value. Therefore, the increase of the piezoelectric and dielectric properties was to be closely related with the increase of P_r.

Acknowledgements

This research was supported by the Program for the Training of Graduate Students in Regional Strategic Industries and Regional Innovation Center (RIC) Program which was conducted by the Ministry of Commerce, Industry and Energy of the Korean Government.

References

[1] J. Long, H. Chen, Z. Meng, Effects of compositions and Nb-doping on microstructure and piezoelectric properties of PMS-PZ-PT system, Mater. Sci. Eng. B B99 (2003) 445–448.
[2] G.M. Lee, Agency for Technology and Standards, Industry and Energy of the Korean Government, in: Seminar on EU Product-Related Regulations, 2004, p. 6.
[3] H. Nagata, T. Takenaka, Additive effects on electrical properties of $(Bi_{1/2}Na_{1/2})TiO_3$ ferroelectric ceramics, J. Eur. Ceram. Soc. 21 (2001) 1299–1302.
[4] G.A. Smolenskii, A.I. Agranovskaya, Dielectric polarization and losses of some complex compounds, Sov. Phys. Tech. Phys. (Engl. Transl.) 3 (1958) 1380–1382.
[5] K. Sakata, Y. Masuda, Ferroelectric and antiferroelectric properties of $(Na_{0.5}Bi_{0.5})TiO_3$–$SrTiO_3$ solid solution ceramics, Ferroelectrics 7 (1) (1974) 347–349.
[6] T. Takenaka, K. Sakata, K. Toda, Piezoelectric properties of $(Bi_{1/2}Na_{1/2})TiO_3$-based ceramics, Ferroelectrics 106 (1) (1990) 375–380.
[7] T. Takenaka, K. Maruyama, K. Sakata, $(Bi_{1/2}Na_{1/2})TiO_3$–$BaTiO_3$ system for lead-free piezoelectric ceramics, Jpn. J. Appl. Phys. 30 (1991) 2236–2239.
[8] H. Nagata, T. Takenaka, Lead-free piezoelectric ceramics of $(Bi_{1/2}Na_{1/2})TiO_3$–1/2(Bi_2O_3·Sc_2O_3) system, Jpn. J. Appl. Phys. (Part I) 36 (1997) 6055–6057.
[9] H. Nagata, T. Takenaka, Lead-free piezoelectric ceramics of $(Bi_{1/2}Na_{1/2})TiO_3$–$KNbO_3$–1/2(Bi_2O_3·Sc_2O_3) system, Jpn. J. Appl. Phys. 37 (1998) 5311–5314.
[10] S. Okamura, S. Miyata, Y. Mizutani, T. Nishida, T. Shiosaki, Conspicuous voltage shift of D–E hysteresis loop and asymmetric depolarization in Pb-based ferroelectric thin films, Jpn. J. Appl. Phys. 38 (1999) 5364–5367.
[11] H. Nagata, N. Koizumi, T. Takenaka, Lead-free piezoelectric ceramics of $Bi_{0.5}Na_{0.5}TiO_3$–$BiFeO_3$, Key Eng. Mater. 169–170 (1999) 37–40.
[12] T. Wada, K. Toyoike, Y. Imanaka, Y. Matsuo, Dielectric and piezoelectric properties of $(A_{0.5}Bi_{0.5})TiO_3$–$ANbO_3$ (A = Na, K) systems, Jpn. J. Appl. Phys. 40 (9B) (2001) 5703–5705.
[13] Y.M. Li, W. Chen, Q. Xu, J. Zhou, H.J. Sun, M.S. Liao, Dielectric and piezoelectric properties of $Na_{0.5}Bi_{0.5}TiO_3$–$K_{0.5}Bi_{0.5}TiO_3$–$NaNbO_3$ lead-free ceramics, J. Electroceram. 14 (1) (2005) 53–58.
[14] R. Zuo, C. Ye, X. Fang, J. Li, Tantalum doped $0.94Bi_{0.5}Na_{0.5}TiO_3$–$0.06BaTiO_3$ piezoelectric ceramics, J. Eur. Ceram. Soc. 28 (4) (2008) 871–877.
[15] B.J. Chu, D.R. Chen, G.R. Li, Q.R. Yin, Electrical properties of $Na_{1/2}Bi_{1/2}TiO_3$–$BaTiO_3$ ceramics, J. Eur. Ceram. Soc. 22 (13) (2002) 2115–2121.
[16] Y. Wu, H. Zhang, Y. Zhang, J. Ma, D. Xie, Lead-free piezoelectric ceramics with composition of $(0.97 - x)Na_{1/2}Bi_{1/2}TiO_3$–$0.03NaNbO_3$–$xBaTiO_3$, J. Mater. Sci. 38 (5) (2003) 987–994.
[17] H. Nagata, M. Yoshida, Y. Makiuchi, T. Takenaka, Large piezoelectric constant and high curie temperature of lead-free piezoelectric ceramic ternary system based on bismuth sodium titanate–bismuth potassium

titanate–barium titanate near the morphotropic phase boundary, Jpn. J. Appl. Phys. 42 (2003) 7401–7403.

[18] L. Wu, D.Q. Xiao, D.M. Lin, J.G. Zhu, P. Yu, Synthesis and properties of $[Bi_{0.5}(Na_{1-x}Ag_x)_{0.5}]_{1-y}Ba_yTiO_3$ piezoelectric ceramics, Jpn. J. Appl. Phys. 44 (2005) 8515–8518.

[19] A. Herabut, A. Safari, Processing and electromechanical properties of $(Bi_{0.5}Na_{0.5})_{(1-1.5x)}La_xTiO_3$ ceramics, J. Am. Ceram. Soc. 80 (11) (1997) 2954–2958.

[20] H.D. Li, C.D. Feng, P.H. Xiang, Electrical properties of La^{3+}-doped $(Na_{0.5}Bi_{0.5})_{0.94}Ba_{0.06}TiO_3$ ceramics, Jpn. J. Appl. Phys. Part I 42 (12) (2003) 7387–7391.

[21] H.D. Li, C.D. Feng, W.L. Yao, Some effects of different additives on dielectric and piezoelectric properties of $(Bi_{1/2}Na_{1/2})TiO_3$–$BaTiO_3$ morphotropic-phase-boundary composition, Mater. Lett. 58 (7–8) (2004) 1194–1198.

[22] X. Zhou, H.S. Gu, Y. Wang, W.Y. Li, T.S. Zhou, Piezoelectric properties of Mn-doped $(Na_{0.5}Bi_{0.5})_{0.92}Ba_{0.08}TiO_3$ ceramics, Mater. Lett. 59 (13) (2005) 1649–1652.

[23] IRE Standards on Piezoelectric Crystals: Measurements of Piezoelectric Ceramics, in: Proceedings of the Institute of Radio Engineers, 49 (7) (1961) pp.1161–1169.

[24] E. Brzozowski, M.S. Castro, Lowering the synthesis temperature of high-purity $BaTiO_3$ powders by modifications in the processing conditions, Thermochim. Acta 398 (1–2) (2003) 123–129.

[25] M.J. O'neil, A. Smith, P.E. Heckeman, J.R. Obenchain, J.A.R. Gallipeau, M.A. D'Arecca, S. Budavari, The Merck Index, Merck & Co., Inc., USA, 2001.

[26] M. Vieth, S. Mathur, N. Lecerf, V. Huch, T. Decker, H.P. Beck, W. Eiser, R. Haberkom, Sol–gel synthesis of nano-scaled $BaTiO_3$, $BaZrO_3$ and $BaTi_{0.5}Zr_{0.5}O_3$ oxides via single-source alkoxide precursors and semi-alkoxide routes, J. Sol–Gel Sci. Technol. 17 (2) (2000) 145–158.

[27] A. Beauger, J. Mutin, J. Niepce, Synthesis reaction of metatitanate $BaTiO_3$, J. Mater. Sci. 18 (10) (1983) 3041–3046.

[28] K. Uchino, E. Sadanaga, T. Hirose, Dependence of the crystal structure on particle size in barium titanate, J. Am. Ceram. Soc. 72 (8) (1989) 1555–1558.

[29] B.D. Begg, E.R. Vance, J. Nowotny, Effect of particle size on the room-temperature crystal structure of barium titanate, J. Am. Ceram. Soc. 77 (12) (1994) 3186–3192.

[30] B.S. Kang, D.G. Choi, S.K. Choi, Effects of grain size on pyroelectric and dielectric properties of $Pb_{0.9}La_{0.1}TiO_3$ ceramic, J. Korean Phy. Soc. 32 (1998) S232–S234.

[31] G. Arlt, The influence of microstructure on the properties of ferroelectric ceramics, Ferroelectrics 104 (1990) 217–227.

[32] K. Uchino, Piezoelectric Actuators and Ultrasonic Motors, Kluwer Academic Publishers, USA, 1997.

[33] W.R. Bussem, L.E. Cross, A.K. Goswami, Phenomenological theory of high permittivity in fine-grained barium titanate, J. Am. Ceram. Soc. 49 (1) (1966) 33–36.

[34] W.R. Bussem, L.E. Cross, A.K. Goswami, Effect of two-dimensional pressure on the permittivity of fine- and coarse-grained barium titanate, J. Am. Ceram. Soc. 499 (1) (1966) 36–39.

[35] G.H. Haertling, W.J. Zimmer, Analysis of hot pressing parameters for lead–zirconate–lead titanate ceramics containing two atom percent bismuth, Am. Ceram. Soc. Bull. 45 (1966) 1084–1089.